JOURNAL OF MATERIALS SCIENCE 33 (1998) 5637–5642

Pitting behavior of SiCp/2024 Al metal matrix composites

Z. FENG*, C. LIN
State Key Laboratory of Physical Chemistry of the Solid Surface, Institute of Physical Chemistry, Department of Chemistry, Xiamen University, Xiamen 361005, China
E-mail: xmums@jingxian.xmu.edu.cn

J. LIN
Department of Materials Science, Shanghai Jiaotong University, Shanghai, China

J. LUO
Department of Chemical and Materials Engineering, University of Alberta, Edmonton, Alberta, Canada

The effects of the volume fraction of SiC particulate reinforcements and the concentration of chloride ions in solution on the localized corrosion characteristics of SiCp/2024 Al metal matrix composites (MMC) were investigated. A scanning micro reference electrode (SMRE) technique was employed to study the dynamic process of pitting initiation and development on the surface of the composites at open-circuit potential. Potentiodynamic polarizations were performed to characterize the electrochemical behavior of the MMCs. The morphology of the localized attack on the MMC sample after corrosion tests were examined by scanning electron microscopy (SEM). The results of electrochemical measurement showed that the composites were less resistant to pit initiation than the corresponding unreinforced metrix alloy. Increase in the volume fraction of SiCp reinforcement in the SiCp/2024 Al composites resulted in a significant decrease of pitting potential. *In situ* potential mapping of active centers on the surfaces of the composites revealed that local breakdown of passivity and initiation of micro pitting corrosion could take place even at an open-circuit potential which was more negative than the pitting potential, and the number of active centers on the surfaces of the composites increased as the volume fraction of SiC particulates in MMCs increased. Micro-structural analysis indicated that pitting attack on the composites mainly occurred at SiCp-Al interfaces or inclusions-Al interfaces.

1. Introduction

With the recent focus on high volume-low cost metal matrix composites (MMCs), the emphasis has shifted towards short fiber or particulate reinforcements [1]. MMCs fabricated with lightweight Al alloy matrices and high modulus SiC reinforcements offer excellent structural properties. However, addition of reinforcements to an aluminum alloy will change the corrosion behavior significantly. Therefore, the attention given to its corrosion behavior has gradually increased in recent years.

Pitting represents one of the most common forms of corrosion for aluminum matrix composites, particularly in solutions containing chloride ions. There is no agreement about the effect of SiC particulate reinforcement on the corrosion behavior of aluminum matrix composites thus far. Previous studies of the corrosion behaviors of SiCp/6061 Al, SiCp/2014 Al, SiCp/2124 Al, and SiCp/A356 Al MMCs in solutions containing chloride ions revealed that the pitting potentials (E_p) of these MMCs were similar to the corresponding unreinforced matrix alloy, and increases in the size or volume fraction of reinforcement did not alter open-circuit potentials (E_{corr}) or pitting potential (E_p) very much [2–6]. However, Trowsdale et al. indicated that SiCp/1050 Al MMCs showed increased susceptibility to pitting attack compared with unreinforced alloys [7]. To the knowledge of the authors, limited information is available regarding the pitting behavior of SiC_p/2024 Al MMCs in sodium chloride solution.

Sun et al. suggested that pitting behavior of MMCs seemed to be controlled by surface films, and film breakdown was related to the volume percentage of SiCp and to NaCl concentration [2]. Therefore, investigation of the effects of composition and microstructure of composites on processes of film breakdown and pitting initiation will contribute to a better understanding of the corrosion mechanism of composites, and the development of techniques for corrosion protection as well. Although the active centers on the surfaces of

* Author to whom all correspondence should be addressed.

MMCs have been located *ex-situ* by using SEM and scanning auger microscopy (SAM) [8, 9], the real-time and *in-situ* identification of the dynamic processes of pit initiation and development can not be achieved by the applications of high vacuum techniques, such as SEM, SAM or conventional electrochemical techniques. Using SMRE, studies were conducted to map *in situ* the initiation and development of active centers at the surfaces of SiCp/2024 Al MMCs. The effects of the volume fraction of SiC particulate in MMCs and the concentration of chloride ions in solutions on the pitting behavior of the composites were determined. Data obtained *in situ* by SMRE were used to correlate the location of pit initiation sites with microstructural features.

2. Materials and methods

Silicon carbide particulate (SiCp) reinforced metal-matrix composites were used in this investigation. The matrix of the composites was a 2024 aluminum alloy, the composition of which is listed in Table I. The composites contained different volume fractions of SiCp ($V_F = 5$, 10, 15, and 20%). The mean size of the SiCp was 14 μm. A 2024 aluminum alloy without silicon carbide particulate ($V_F = 0\%$) was used for comparison. The preparation of the composites has been reported elsewhere [10]. Rectangular specimens with an area of 8×6 mm^2 and 5 mm in thickness were sectioned from the bulk using a wire saw. An insulated Cu wire, 0.8 mm in diameter, was soldered to each specimen as a lead. The specimens were then embedded in epoxy, leaving only one of the surfaces exposed to the solution. The testing surfaces of the specimens were mechanically ground, using 320, 400, and 600 grade silicon carbide paper progressively followed by polishing with 6-μm and 1-μm diamond suspensions. The specimens were ultrasonically cleaned in acetone and distilled water, and then stored in a desiccator before testing.

TABLE I Composition of the 2024 aluminum matrix (wt%)

Cu	Mg	Mn	Al
3.8–4.9	1.2–1.8	0.3–0.9	rest

Solutions of 0.01, 0.1, and 0.5 M NaCl were prepared with analytical grade NaCl and distilled water. The pH of the solutions was near neutral. A Model 273 PAR potentiostat/galvanostat was used in the experiments. The potentials were measured versus a saturated calomel reference electrode (SCE). Cyclic potentiodynamic anodic polarization was carried out on SiCp/2024 Al MMCs and 2024 aluminum alloy, respectively. Steady corrosion potentials (E_{corr}) were obtained after approximately two hours for the specimens in solutions. The polarization scan started at -800 mV, proceeded upward to a final anodic current density of approximately 500 μA/cm^2, and then reverted to -800 mV. E_p was characterized by a sudden rise in current and was interpreted as the onset of stable pitting. Repassivation potential (E_{prot}) was taken as the crossover point of the curves for foward scan and reverse scan. The solutions were open to air. The scan rate was 0.2 mV/s. At least four specimens were tested for each testing condition to determine the mean values of E_p, E_{prot} and E_{corr}.

A scanning micro-reference electrode imaging system established in our laboratory was employed in this investigation [11]. The principles of the scanning micro reference electrode (SMRE) imaging system have been illustrated by Isaacs and Vyas [12]. Its schematic diagram is shown in Fig. 1. A PC-based system was developed to control positioning and scanning of the microelectrode over the specimen surface, data acquisition and image representation. The scanning device of the system was driven by two stepper motors that manipulated both the specimen and the micro electrode. The maximum range of the scan was 25×15 mm with an increment of 50 μm for each step. Either a 3-dimensional stereo map or equipotential contour can be chosen for data representation. The configuration of the scanning

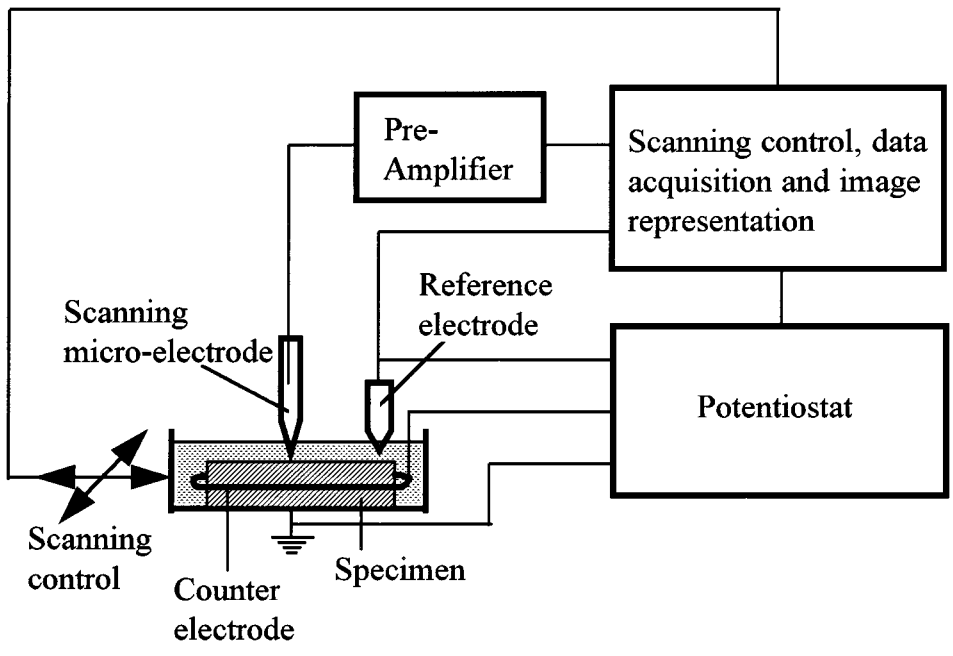

Figure 1 Schematic of the scanning micro-reference electrode imaging system.

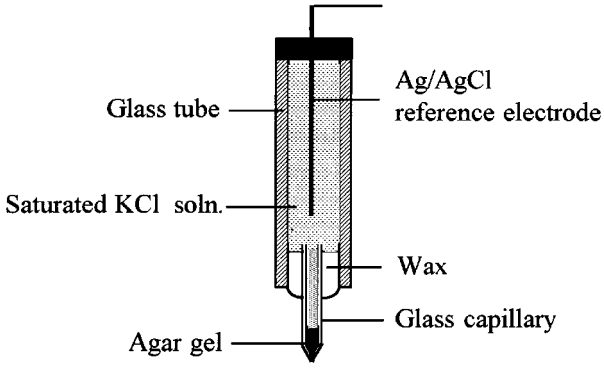

Figure 2 Details of the scanning micro-reference electrode.

micro reference electrode is shown schematically in Fig. 2. It consisted of a Pyrex glass capillary having a tip of 10-20 μm in diameter, which was fused to a large-diameter glass tube using molten wax. The glass capillary was filled with 1 M KCl solution containing agar gel. The glass tube was filled with saturated KCl solution to create a salt-bridge-type arrangement. An Ag/AgCl reference electrode was placed in the solution at the top end of the glass tube.

A polished specimen was installed face upward onto the scanning stage of the device. The positioning of the tip of the microprobe with respect to the surface of a specimen was conducted by a manual micrometer under a 10 $\times$ optical microscope to achieve a vertical distance of approximately 10 μm. Solutions of 0.1 M NaCl were then poured into the cell. Testing was conducted at open-circuit potential. All the SMRE scans were taken at about 25 °C.

The examination of the pit morphology and chemical composition of microstructural features of the MMCs was then performed using a scanning electron microscope (Hitachi S-520) and an energy dispersive spectroscope (EDAX9100).

3. Results

3.1. Electrochemical experiments

The mean values of pitting potential E_p, repassivation potential E_{prot}, and steady corrosion potential E_{corr} are shown in Table II. Effects of the volume fraction of SiC particulate (V_F) on the E_p of the composites were demonstrated to be significant. E_p decreased as the volume fraction of SiC particulate reinforcement increased. The correlation between E_p and V_F of the composites in 0.01, 0.1, and 0.5 M NaCl solutions were shown to be statistically significant ($p < 0.004$ for all). In general, E_p decreased as the concentration of chloride ions in solution increased. However, there was no statistically significant correlation between E_p and the concentration of Cl^- in solution ($p > 0.2$ for all). There was no statistically significant correlation between repassivation potential E_{prot} and volume fraction of SiCp reinforcements V_F of the composites either.

TABLE II Summary of electrochemical tests

	E_p (mV)			E_{prot}(mV)			E_{corr} (mV)
SiC V_F-%	0.01 M NaCl	0.1 M NaCl	0.5 M NaCl	0.01 M NaCl	0.1 M NaCl	0.5 M NaCl	0.1 M NaCl
0	−430	−497	−565	−653	−620	−612	−574
5	−460	−528	−597	−750	−700	−670	−610
10	−485	−555	−625	−740	−765	−725	−688
15	−538	−632	−662	−700	−720	−750	−671
20	−550	−650	−692	−670	−720	−775	−671

3.2. Scanning micro-reference electrode experiments

After the Al MMC specimens were immersed in 0.1M NaCl solution, the open-circuit potential increased gradually at first, then decreased to a stable value. However, the drift of open-circuit potential never was beyond the region between E_p and E_{prot}. It took approximately 150 to 240 minutes for the open-circuit potentials to reach a stable value. SMRE scans taken during this period often gave good indications of the dynamic process of initiation and development of micropitting. Fig. 3 shows the varieties of potential distribution and height of the peaks at the surfaces of the SiCp/2024 Al composites ($V_F = 5\%$ and 15%) measured after different immersion times in 0.1 N NaCl solution (30, 90, and 150 minutes). A peak appearing on the potential map might not represent a single active center, but sometimes represented a local region containing several active centers which were close to each other. The height of the peaks represented the mean speed of corrosion of the local position. The micropit may not always develop into a large pit. Some of the micropits may initiate and cease instantaneously, and some of the micropits may continue to grow for a longer time under a favorable condition. Increase in the volume fraction of SiC particulate reinforcement of the composites resulted in an increase in the number of the potential peaks on the sample surfaces. The appearance of the mapping of active centers on the electrode surface was consistent with the variation of open-circuit potential. Right after immersion of an electrode into the NaCl solution, a few peaks could be found on its surface. The height of the peaks was relatively low, but increased with time. At about 90 to 120 minutes after immersion of the specimen into the NaCl solution, the height of the peaks on the electrode surface reached the maximum. Thereafter, the height of the peaks decreased with time. After about 150 to 240 minutes of immersion, the height of the peaks tended to maintain a stable value, which was normally lower than the maximum value and higher than the value during the initiation period. During the whole process, some peaks continued to develop as others subsided. The maximum height of the peaks did not change significantly with the change in the volume fraction of SiCp in the MMCs.

SEM and EDAX examination revealed that pitting corrosion attack on unreinforced Al 2024 alloy occurred at the Al-inclusions interfaces. As for SiCp/2024 Al composites, pitting corrosion attack occurred preferentially at the SiC-Al interfaces (Fig. 4a) and Al-inclusions interfaces (Fig. 4b). It was shown that these inclusions were intermetallic compounds

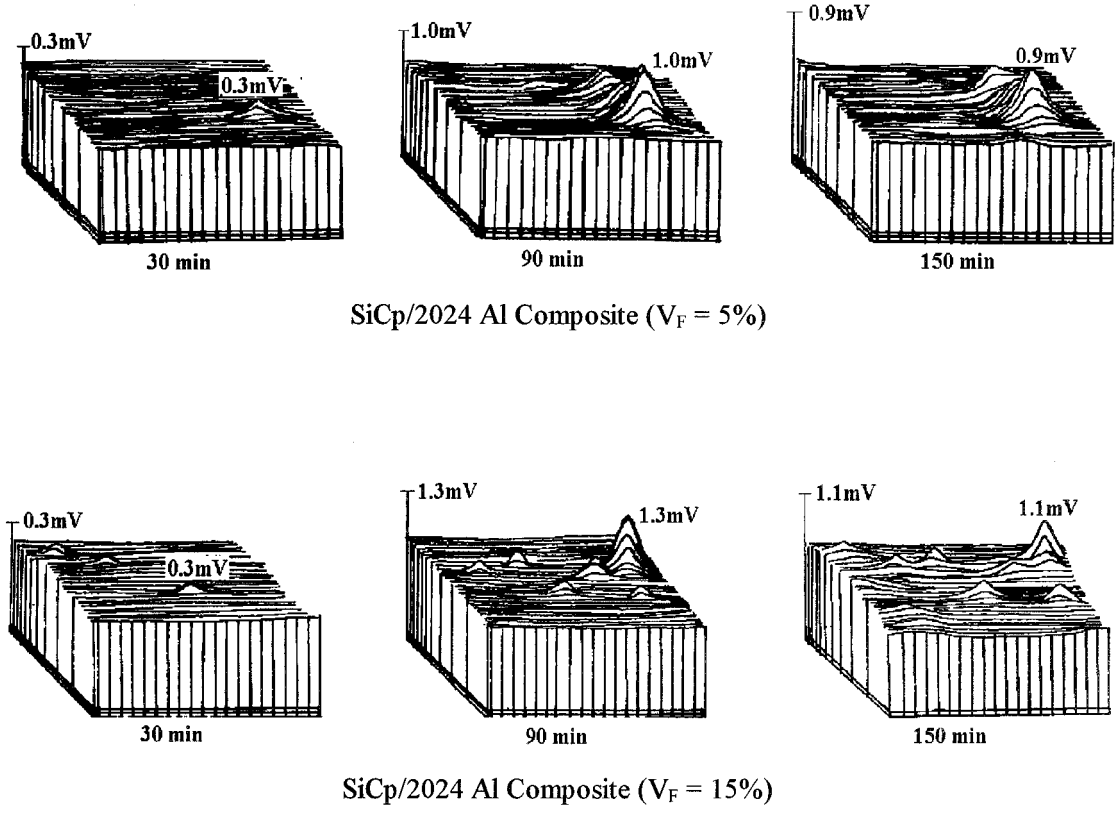

Figure 3 Potential distribution on surfaces of the SiCp/2024 Al composites in 0.1 M NaCl solution at open-circuit potential.

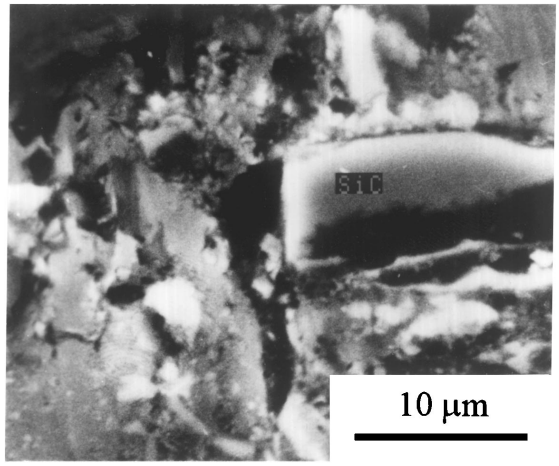

(a)

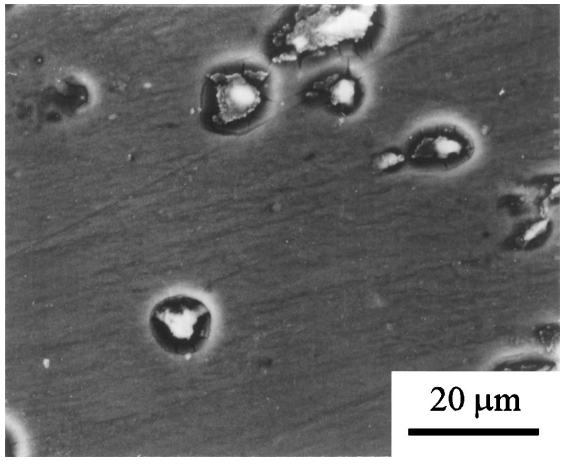

(b)

Figure 4 Scanning electron micrographs of pits on interfaces of (a) SiCp-2024 Al matrix, and (b) inclusions-2024 Al matrix.

composed of alloying element of Cu and Al (Fig. 5a), or Cu, Mn, Al, as well as Fe (Fig. 5b).

4. Discussion

The experiments showed that addition of SiC particles to 2024 aluminum alloy significantly affected the corrosion behavior of the composite. The trend was in agreement with Trzaskomas' report, that SiC_w/2024 Al composite showed a greater susceptibility to pit initiation than unreinforced 2024 aluminum alloy [13]. The difference between this study and Trzaskoma's is that the reinforcement of the MMCs used in this study consisted of SiC particulates instead of SiC whiskers. In addition, the effects of the volume fraction of SiC particulate reinforcements and the concentration of chloride ions in solution on the pitting behavior of SiCp/2024 MMCs were investigated as well. To the knowledge of the authors, this report may be the first one with respect to the investigation of the pitting behavior of SiCp/2024 Al composites using SMRE.

The real time *in situ* investigation on the pitting behavior of SiCp/2024 Al MMCs using the SMRE technique provided the dynamic information of pit initiation and development. SMRE has been demonstrated to have the characteristics of high sensitivity and direct mapping of active centers on the surface of an electrode with a two-dimensional resolution of micrometers. Our study reveals that even at the open-circuit potentials which are more negative than corresponding pitting potentials E_p, there exists a process of localized micropitting. This result is consistent with the previous discovery that the E_p potential may not actually be the characteristic potential for passivity breakdown and

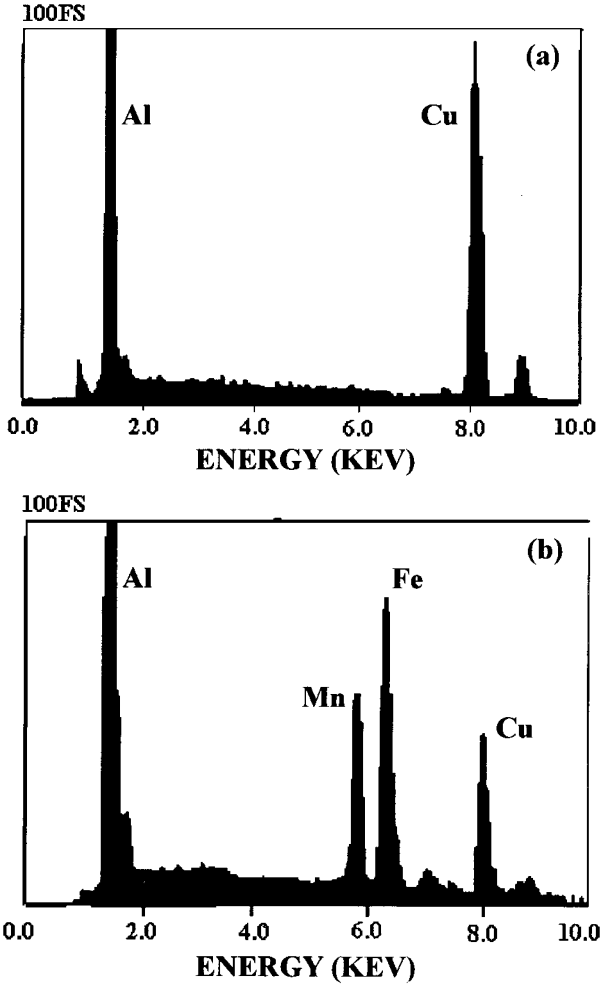

Figure 5 EDAX spectrum of (a) Al_2Cu and (b) (CuFeMn) Al_6 inclusions.

micropitting initiation. It may be explained as a critical potential characterizing pit propagation, and at E_p potential the pit may continue to develop to a visible pit if the condition is maintained [14]. However, the SMRE *in situ* measurements revealed that unlike the micropitting on the surface of stainless steel, the micropits on the surface of aluminum MMCs usually developed once initiated, though height of the peaks will change with time. The phenomenon suggests that the oxide film on the surface of MMCs can hardly be repassivated after localized corrosion is initiated.

It is generally accepted that the following steps are involved in the initiation of localized corrosion of aluminum alloy: adsorption of the reactive anion on the oxide-covered aluminum, chemical reaction of the adsorbed anion with the aluminum ion in the aluminum oxide lattice or the precipitated aluminum hydroxide, thinning of the oxide by dissolution, and direct attack of the exposed metal by the anion [15]. The corrosion characteristics of SiC_p/2024 Al metal matrix composites can be considered from the effects of composition as well as its microstructure. In general, the adsorption of Cl^- on oxide-coated aluminum might be nonuniform. It is reasonable to expect enhanced adsorption and surface activity at the imperfection or flaw in the oxide film. When a certain Cl^- concentration is reached, the local oxide film which is weakest will be thinned by dissolution. As a result, the increase of Cl^- in solution may aggravate Cl^- adsorption and accumulation onto the preferential sites on the surface of composites, and result in initiation of micropitting. SiC particulate reinforcement not only leads to imperfection of the oxide film [2], it may also change the kinetics of the precipitation of the second phase in the matrix to cause a change in the microstructure of the MMCs. The latter will change the mechanics of initiation of pitting [3]. Although Hihara and Latanision showed no significant enhancement of the corrosion rate due to the SiC/Al couple [16], the SiCp-Al interface will act as an active region for the following reasons: First, the thermal expansion coefficient of SiC is significantly lower than that of aluminum alloy. As the composites cool from melting temperature, the great difference in the thermal expansion coefficients between SiC and the aluminum matrix will result in a high density of dislocation at SiC-Al interface. The bigger the SiC particles, the higher the density of dislocation. An increase of dislocation density in the matrix with the addition of SiC particulate reinforcement in SiCp/2024 Al composites has been demonstrated [10]. That region can act as an active center as the MMCs are immersed in NaCl solution. Second, the addition of SiCp reinforcement introduced precipitation of Al_2CuMg and Al_2Cu, or segregation of Mg to the SiC-Al interface [10]. The Mg-rich interface provided a nucleation site for localized corrosion by forming a local galvanic cell with the adjoining Al matrix [17]. Due to the increased copper (Cu) precipitation to the interface of SiCp-Al, a matrix of Al containing less Cu will be more sensitive to pitting corrosion [18] (Table III). In addition, as seen in Table III, the open-circuit potentials for Al_2Cu and Al_2CuMg are different from that of aluminum alloy. Therefore, they would behave as a local anode or cathode. In either case, galvanic corrosion will develop and lead to localized corrosion at the SiCp-Al interface.

In addition, the aluminum/silicon carbide interface in the MMCs will provide numerous microcrevice sites. Those sites are potential locations for the development of localized attacks. There is a restricted oxygen supply inside the crevice areas. These areas become the anode, and the passive surface outside the crevice area become the cathodic areas. Once the localized attack is initiated, the dissolved metal cations inside the crevice will produce protons through the hydrolysis process. This will increase the acidity of the crevice electrolyte and

TABLE III Open-circuit potentials for Al-Cu Alloys exposed to 0.1 M NaCl [18]

Alloy or Intermetallic	E_{corr} (mV)
Al + 4% Cu	−690
$CuAl_2$	−730
Al + 2% Cu	−750
99.5% Al	−850
Al + 3% Mg	−870
Al + 7% Mg	−890
Al_2CuMg	−1000

enhance the anodic dissolution. At the same time, chloride ions will migrate under the electric field towards the crevice area and increase the chloride ion concentration. The increase in chloride ion concentration will increase the activity of the protons and further decrease the solution pH. This will start an auto-catalytic process of localized attack. The crevice corrosion mechanism can be applied to the localized corrosion of MMCs in aerated chloride containing solutions.

5. Conclusions

(1) SMRE *in situ* measurements revealed that there were inherent active centers on the surface of SiCp/2024 Al MMCs for localized corrosion initiation. Localized corrosion initiated immediately after immersion in an aerated chloride containing solution and reached a steady development in about two hours at open-circuit potential.

(2) SiCp/2024 Al MMCs showed increased susceptibility to pitting attack compared with unreinforced alloy in NaCl solution. Increase in the fraction of SiCp reinforcement resulted in a significant decrease in pitting potential E_p.

(3) Local breakdown of passivity on the surface of SiCp/2024 Al MMCs and initiation of micropitting may take place even at an open-circuit potential which was more negative than pitting potential E_p. The number of active centers on the surfaces of the composites increased as the volume fraction of SiCp reinforcement increased. These characteristics implied that the localized corrosion of SiCp/2024 Al composites may have resulted from microcrevice corrosion.

(4) The predominant sites for initiation of micropitting on the surface of SiCp/2024 Al MMCs were the interfaces of SiCp-Al or Al-inclusions, which were intermetallic compounds composed of Cu and Al, or Cu, Al, Mn as well as Fe. SiCp particulate reinforcements acted as an active center mainly due to the precipitation of intermetallic compounds or the element Mg to SiCp-Al interface.

Acknowledgements

The financial supports from the National Science Foundation of China, State Key Laboratory for Physical Chemistry of the Solid Surface, Xiamen University and the Natural Sciences and Engineering Research Council of Canada are gratefully acknowledged.

References

1. K. A. LUCAS and H. CLARKE, in "Corrosion of aluminum-based metal matrix composites" (Research Studies Press Ltd., Somerset, England, 1993) p. 6.
2. H. SUN, E. Y. KOO and H. G. WHEAT, *Corrosion* **47** (1991) 741.
3. M. M. BUARZAIGA and S. J. THORPE, *Corrosion* **50** (1994) 176.
4. G. W. ROPER and P. A. ATTWOOD, *J. Mater. Sci.* **30** (1995) 898.
5. P. C. R. NUNES and L. V. RAMANATHAN, *Corrosion* **51** (1995) 610.
6. S. L. COLEMAN, V. D. SCOTT and B. MCENANEY, *J. Mater. Sci.* **29** (1994) 2826.
7. A. J. TROWSDALE, B. NOBLE, S. J. HARRIS, I. S. R. GIBBINS, G. E. THOMPSON and G. C. WOOD, *Corros. Sci.* **38** (1996) 177.
8. P. P. TRZASKOMA, *Corrosion* **46** (1990) 402.
9. J. E. CASTLE, L. SUN and H. YAN, *Corros. Sci.* **36** (1994) 1093.
10. J. S. LIN, P. X. LI and R. J. WU, *Scr. Metall. Mater.* **28** (1993) 281–286.
11. C. J. LIN, Ph.D. Thesis, Xiamen University, 1985.
12. H. S. ISAACS and B. VYAS, in "Electrochemical Corrosion Testing" (ASTM STP 727, 1981) p. 3.
13. P. P. TRZASKOMA, E. MCCAFFERTY and C. R. CROWE, *J. Electrochem. Soc.* **130** (1983) 1804.
14. C. J. LIN and Z. W. TIAN, *Acta Physico-Chimica Sinica* **3** (1987) 479.
15. R. T. FOLEY, *Corrosion* **42** (1986) 277.
16. L. H. HIHARA and R. M. LATANISION, *Corrosion* **48** (1992) 546.
17. E. H. HOLLINGSWORTH and H. Y. HUNSICKER, in "Metals Handbook" (ASM, 1987) **13** p. 583.
18. J. F. MCLNTYRE, R. K. CONRAD and S. L. GOLLEDGE, *Corrosion* **46** (1990) 902.

Received 31 August 1997
and accepted 15 July 1998